Barnett, J. B., Michalis, C., Scott-Samuel, N. E., & Cuthill, I. C. (2018). Distance-dependent defensive coloration in the poison frog *Dendrobates tinctorius*, Dendrobatidae. *Proceedings of the National Academy of Sciences of the United States of America*, *115*(25), 6416-6421. [201800826]. https://doi.org/10.1073/pnas.1800826115

Authors copy of paper in *Proceedings of the National Academy of Sciences USA* (accepted 14/05/18)

Title: Distance-dependent defensive coloration in the poison frog *Dendrobates tinctorius*, Dendrobatidae.

Short title: Distance-dependent color in *Dendrobates tinctorius*

James B. Barnett[a,1], Constantine Michalis[a], Nicholas E. Scott-Samuel[b], Innes C. Cuthill[a,2]

[a]School of Biological Sciences, University of Bristol, Bristol Life Sciences Building, 24 Tyndall Avenue, Bristol, BS8 1TQ, United Kingdom.

[b]School of Experimental Psychology, University of Bristol, 12a Priory Road, Bristol, BS8 1TU, United Kingdom.

Keywords:

acuity | aposematism | camouflage | Dendrobatidae | distance

[1]Present address: Redpath Museum, McGill University, 859 Sherbrooke Street West, Montreal, QC, H3A 0CA, Canada.

[2]To whom correspondence should be addressed. Email: i.cuthill@bristol.ac.uk.

Abstract

Poison dart frogs provide classic examples of warning signals: potent toxins signaled by distinctive, conspicuous coloration. We show that, counterintuitively, the bright yellow and blue-black color of *Dendrobates tinctorius* (Dendrobatidae) also provides camouflage. Through computational modeling of predator vision, and a screen-based detection experiment presenting frogs at different spatial resolutions, we demonstrate that at close range the frog is highly detectable, but from a distance the colors blend together, forming effective camouflage. This result was corroborated with an *in situ* experiment, which found survival to be background dependent: a feature more associated with camouflage than aposematism. Our results suggest that in *D. tinctorius* the distribution of pattern elements, and the particular colors expressed, act as a highly salient close range aposematic signal, while simultaneously minimizing detectability to distant observers.

Significance

Poison dart frogs are well known for their deadly toxins and bright colors: they are a classic example of warning coloration. But conspicuousness is not the only consideration: defensive coloration must be effective against a diverse predator community with a variety of different visual systems, and variable knowledge of prey defenses and motivation to attack. We found that the bright colors of *Dendrobates tinctorius* are highly salient at close-range but blend together to match the background when viewed from a distance. *Dendrobates tinctorius* combines aposematism and camouflage without necessarily compromising the efficacy of either strategy, producing bright colors while reducing encounters with predators. These data highlight the importance of incorporating viewing distance and pattern distribution into studies of signal design.

\body **Introduction**

Poison dart frogs (Dendrobatidae) are well known for their striking aposematic (warning) signals: distinctive, conspicuous coloration signaling potent toxins (1, 2). Predators learn the association between prey coloration and toxic defense, and bright and highly contrasting color patterns have been demonstrated to increase the speed, accuracy, and longevity of predator avoidance learning (3-5).

Aposematic species are not, however, immune to predation (6-10). Naïve and specialized predators will ignore warning coloration, and even susceptible predators will actively manage their intake of defended prey in accordance with their nutritional requirements and toxin burden (6-10). For example, birds and snakes have been observed predating toxic dendrobatid (*Dendrobates, Phyllobates, and Oophaga* spp.) frogs (11-13). Consequently, maximizing detectability is not necessarily the optimal strategy for preventing predation, and defended species may benefit from incorporating aspects of camouflage into their coloration (14-20).

Indeed, rather than being alternative and mutually exclusive forms of defensive coloration, camouflage and aposematism are now frequently considered along a continuum from inconspicuous to highly salient (21). Defended prey trade off the benefits of conspicuous warning signals against a low predator encounter rate, frequently resulting in weaker defenses being associated with smaller and less saturated aposematic components (20, 22, 23). An alternative, which can maintain color saturation and signal size, is aposematic signals which may also act as context-dependent disruptive camouflage (24) or distance-dependent background matching (14, 21).

Disruptive coloration breaks up the outline of a target into unrecognizable patches which blend into different background components (25). As both aposematic and disruptive patterns benefit from highly contrasting colors (3, 5, 26, 27), and disruption does not necessarily require that colors match the background (28), there is potential for cooption of similar pattern components despite the opposing processes (21). However, whereas consistent symmetrical patterns are more easily learned and

remembered (29), asymmetric and variable patterns are more effective at concealing prey (26, 30, 31). It has been demonstrated that conspicuous warning signals can appear cryptic in particular microhabitats (24), but it is unknown how widespread this mechanism is in nature.

Distance-dependent patterns, on the other hand, take advantage of limitations in observer visual acuity to appear highly salient at close range, but camouflaged when viewed from a distance (15, 16, 18, 19, 32, 33). This effect can be achieved by either combining patterns of different spatial frequency (size) (18) or by the color components blending together to form a cryptic average color (pattern blending) (19, 32, 33). Previous work using artificial prey suggests that pattern blending can have greater survival than either camouflage or aposematism alone (18, 19). However, although these model systems take inspiration from ecologically relevant patterning, little work has been done into naturally occurring color patterns (15, 16, 32).

Dendrobates tinctorius (Dendrobatidae) is a brightly colored frog found across the Guiana Shield. At the Nouragues Natural Reserve, French Guiana, the frogs are blue-black with a bright yellow ring, which may be broken or joined to form a figure eight (Fig. 1A) (34). However, the presence of asymmetry and variation between individuals does not conform to standard aposematic theory (34, 35), and is reminiscent of cryptic patterning (29). To examine the optical processes involved in the coloration of *D. tinctorius*, we ran computational models of predator vision, an *in situ* survival experiment with the frogs' wild avian predators, and a computer-based detection experiment with human surrogate predators, where we manipulated coloration, patterning, and viewing distance.

Results

Visual modeling. We photographed adult *D. tinctorius* (n = 84) *in situ* near the Saut Pararé camp in the Nouragues Natural Reserve, French Guiana (Fig. 1A). Detectability at different viewing distances was assessed using models of tetrachromatic bird (both violet (VS) and UV sensitive), trichromatic snake, dichromatic mammal, and trichromatic human visual perception. The avian, snake, and mammalian

89 models are representative of potential visual predators of dendrobatid frogs (11-13, 36), and we included
90 human vision to allow intuitive interpretation of the results.

91 Support Vector Machines (SVM) (37) were used as a classifier, and discrimination accuracy (frog vs leaf
92 litter background) was assessed using the Area Under the Curve (AUC) of Receiver Operated
93 Characteristic (ROC) curves (38). An AUC of 1.0 represents perfect classification whereas an AUC of 0.5
94 indicates random chance. We followed a commonly used grading system interpreting AUC results as: 1.0-
95 0.9 = excellent, 0.9-0.8 = good, 0.8-0.7 = fair, 0.7-0.6 = poor, 0.6-0.5 = fail (39). Data available in the
96 University of Bristol Research Data Repository (40).

97 With all spatiochromatic information, representing close-range viewing, all visual systems were *excellent*
98 at discriminating frog from background (Table 1; Fig. S1). Classification accuracy did, however, change
99 at different spatial resolutions, and the frogs' color and visual texture converged with that of the
100 background at greater viewing distances (Fig. 1B-D). For all visual systems, color discrimination
101 accuracy decreased from *good* at the highest resolution (Very High), to *fair* at low resolution (Low), and
102 *poor* for the mean color, with the dichromatic mammalian model having the largest decline in accuracy as
103 resolution decreased (Table 1; Fig. S2). Similarly, the accuracy of visual texture discrimination declined
104 at lower resolutions, where all visual systems were *good* at the highest resolution but failed to classify
105 effectively at the low resolution (Table 1; Fig. S3).

106 **Survival.** Camouflage is largely background dependent, with even small deviations away from
107 background color and texture leading to significant decreases in survival (41), whereas conspicuous
108 aposematism is more resilient to variation in background coloration (42).

109 To assess how dependent the survival of *D. tinctorius* was on the visual characteristics of the natural
110 background, we used plasticine model frogs to record avian predation, and manipulated both frog color
111 pattern and background. Three different frog colors were designed to represent i) the natural phenotype
112 (N: yellow-and-black), ii) aposematism (Y: plain yellow), and iii) camouflage (C: brown-and-black).

These frogs were presented on four backgrounds: the natural leaf litter (NL), two manipulated backgrounds which differed in color and visual texture from the natural background (plain soil (NS) and a homogeneously colored paper square (PA)), and a paper square printed with leaf litter (PL) which acted as a control for the use of paper backgrounds (Fig. S4).

We found a significant interaction between frog color pattern and background type ($\chi^2 = 50.67$, d.f. = 11, $P < 0.001$), so each frog color was analyzed separately. There was a significant effect of background on the survival of the brown-and-black frogs ($\chi^2 = 29.35$, d.f. = 3, $P < 0.001$). There was no significant difference in survival between the natural background (NL) and the printed leaf litter (PL) background (CNL-CPL: $z = 1.45$, $P = 0.150$), but the brown-and-black frogs had significantly higher survival on leaf litter than on both the modified backgrounds (CNL-CNS: $z = 3.10$, $P = 0.002$; CNL-CPA: $z = 4.40$, $P < 0.001$; Fig. 2 left). Conversely, there was no significant effect of background on the survival of plain yellow frogs ($\chi^2 = 0.51$, d.f. = 3, $P = 0.918$; all pairwise tests: $z < 0.62$, $p > 0.540$; Fig. 2 middle). These results are consistent with the brown-and-black frog being camouflaged on the leaf litter and the plain yellow being equally detectable on all backgrounds. This conclusion is further supported by visual modeling of the stimuli photographed *in situ* (Fig. S5).

We found a significant effect of background on the yellow-and-black frogs which mimicked the natural phenotype ($\chi^2 = 12.10$, d.f. = 3, $P = 0.007$). There was no significant difference between leaf litter backgrounds (NNL-NPL: $z = 0.72$, $P = 0.470$), but survival was significantly higher on the natural background than on modified backgrounds (NNL-NNS: $z = 2.44$, $P = 0.015$; NNL-NPA: $z = 2.90$, $P = 0.004$; Fig. 2 right). The survival of the yellow-and-black phenotype, therefore, appears to be dependent on the visual characteristics of the background in a similar manner to the brown-and-black frog, but counter to the plain yellow frog.

Detection. To investigate further how viewing distance affects the detectability of *D. tinctorius*, we performed a screen-based detection experiment with human participants (n =18). We manipulated frog

coloration (Fig. S6), and presented the stimuli on their natural leaf litter background under conditions representing three viewing distances: Near, Medium, and Far. The human participants were required to click on the frogs, and we recorded both reaction time (Table 2; Fig. 3) and detection accuracy.

Reaction time. We found a significant interaction between frog coloration and distance ($\chi^2 = 1670.40$, d.f. = 22, $p < 0.001$), and so treatment effects were analysed separately for each distance. At close-range (Near) we found that the natural yellow and blue-black pattern (A) was detected significantly more slowly than plain yellow (C<A) and reverse color pattern (D<A) frogs, both of which increased the proportion of yellow, but the natural pattern was detected significantly faster than plain blue-black (A<B). At long distances (Far), however, it took participants significantly longer to detect the natural pattern compared to the plain yellow (C<A), reversed pattern (D<A), and the plain blue-black (B<A).

The magnitude of these effects shows that at close-range the natural pattern grouped more readily with the conspicuous high yellow patterns (C and D) than the more cryptic plain blue-black (B). However, when viewed from a greater distance, the time taken to detect the natural pattern greatly increased, and the natural pattern grouped more readily with cryptic patterns. At the furthest distance the natural pattern provides more effective camouflage than the plain blue-black (B<A; Table 2; Fig. 3).

The arrangement of the natural pattern also appears well suited for both short-range detectability and long-range camouflage. At close-range, rearranging the pattern, while maintaining the ratio of color components, could increase but not decrease reaction time (A=E and A<F), whereas at long-range we found the opposite (E<A and A=F). We therefore conclude that the pattern is arranged to be highly salient at close range but cryptic when viewed from a distance.

Moreover, we found no evidence of disruptive camouflage, which would predict that high contrast patterning would increase reaction time when compared to plain colors (26, 30). In contrast, when comparing frogs with brown rather than yellow patterning to plain brown or black frogs, we found that the presence of patterning decreased reaction time at close-range (G<B and H<J) and had no effect at

greater distances (G=B and H=J). These data suggest that at close range the pattern itself acts as a salient signal even in the absence of conspicuous coloring.

Furthermore, our data suggest that, when viewed from a distance, the yellow and blue-black components are spatially averaged to produce a mean color which provides effective camouflage. As distance increases, the time taken to detect the natural pattern (A) converges with that of its mean color (I), and at greater viewing distances the mean color is just as effective as the average color of the background (J) and random-sample background matching (K) at preventing detection.

Detection accuracy. A similar trend was observed in the detection accuracy data. There was a significant interaction between treatment and distance ($\chi^2 = 297.64$, d.f. = 22, $P < 0.001$), and so each distance was analyzed separately. We found a significant effect of treatment at the Near ($\chi^2 = 249.26$, d.f. = 11, $P < 0.001$) and Medium ($\chi^2 = 675.05$, d.f. = 11, $P < 0.001$) distances, but detection accuracy was too high for reliable pairwise tests.

At the furthest distance (Far) there was a significant effect of treatment ($\chi^2 = 2769.10$, d.f. = 11, $P < 0.001$) and pairwise tests were possible. Increasing the amount of yellow in the pattern (C and D) increased detection accuracy over the natural pattern (A<C: $z = -8.49$, $P < 0.001$; A<D: $z = -15.64$, $P < 0.001$), as did rearranging the pattern into a signal yellow circle (A<E: $z = -15.40$, $P < 0.001$). Whereas there was only a marginal effect of moving the yellow pixels to highlight the edge of the frog (E<A: $z = -2.66$, $P = 0.076$). Furthermore, the natural pattern was detected more accurately than the mean color of the frog (I<A: $z = -8.57$, $P < 0.001$) and the unmanipulated frog (L<A: $z = -6.93$, $P < 0.001$). No further pairwise tests were significant ($z < 2.15$, $P > 0.265$).

Discussion

Aposematic signals are made up of both color and visual texture information. However, whereas color saturation has been studied in detail, patterning has received comparatively little attention. Most research

184 into pattern has focused on close-range signaling properties and suggests that high contrast patterns can
185 increase the saliency, memorability, and consistency of a signal (3-5). Alternatively, however, it has been
186 suggested that high contrast patterning may reduce detectability, through either disruptive camouflage
187 (24) or distance-dependent signaling (14-20).

188 Taken together, our data suggest that *D. tinctorius* displays a specific ratio and distribution of color
189 components which combines highly salient aposematic signaling with effective and targeted background
190 matching camouflage. At close-range the pattern is easily detectable, utilizing bright colors not found in
191 the background to increase color contrast. At greater viewing distances, these highly contrasting colors
192 merge together to form an average which closely matches that of the background, such that the time taken
193 to detect the average color of the frog cannot be distinguished from that of background matching
194 camouflage.

195 Moreover, at close-range the pattern of *D. tinctorius* is distinct from the textural component of the
196 background and appears to act as a salient signal even in the absence of conspicuous coloring. At long-
197 range, in a similar manner to color-blending, textural information converges to match that of background.
198 We therefore found no evidence to support disruptive camouflage but, rather, these data are consistent
199 with distance-dependent pattern blending (19, 32, 33). This result is consistent for avian, snake, mammal,
200 and human visual perception, and translates into a decrease in avian predation on the frog's natural
201 background.

202 The bright colors of *D. tinctorius* have previously been associated with aposematism (43, 44) and sexual
203 signaling (34). Brighter and more conspicuous signals have been demonstrated to improve the efficacy of
204 aposematism (45, 46) and to be favored during mate selection in dendrobatid frogs (47, 48). Under natural
205 conditions, however, variation in predator motivation towards aposematic prey means that incorporating
206 aspects of camouflage may increase survival (6-10, 20). Indeed, even in the absence of aposematic
207 defense, distance-dependent patterning may facilitate the greater color saturation favored for mate

attraction without necessarily increasing predation risk, especially where conspecifics and predators operate on different spatial scales.

It has further been suggested that the colors of *D. tinctorius* may disrupt a predator's ability to track a moving frog (motion dazzle) (49, 50) and that phenotypic variation may trade-off the benefits of salient signaling versus camouflage (35). We propose pattern-blending as an additional (albeit not mutually exclusive) optical mechanism which combines the benefits of both salient signaling and camouflage; reducing predator encounter rates while retaining effective aposematism (18).

Evidence for distance-dependent signaling from natural phenotypes is currently scarce, with most research focusing on predominantly cryptic patterns with small aposematic components (15, 16). In contrast, the yellow and blue-black of *D. tinctorius* does not appear to share features usually indicative of camouflage, and our data highlight how patterning and background characteristics may influence saliency and detectability.

The particular balance between aposematism and camouflage, may be affected by differences in toxin susceptibility between different predators, or temporal shifts in the predators' motivation to attack. Predator motivation may vary considerably due to seasonal differences in community composition, competition, energetic requirements, and the availability of alternate prey (6, 51), whereas predation risk may also fluctuate as dietary derived toxicity and the frog's level of activity may shift with changing environmental conditions (52-54).

Indeed, different components within the coloration of *D. tinctorius* may fulfil different roles and be individually selected (55). More research is needed to understand how multiple functions interact under different viewing conditions (e.g. lighting conditions (35) / viewing distance and angle), in different contexts (e.g. microhabitats (35) / posture and motion (49, 50)), and to different observers (predators and conspecifics), as well as how color is affected by temporal changes in behavior, toxicity, and the visual environment. Furthermore, intraspecific variation both within (seemingly continuous) (35, 49) and

between (largely discrete) (43, 44, 55, 56) populations suggests this balance in selection pressures may vary both geographically and between individuals. Although it is currently unknown whether these differences are the result of natural or sexual section, or neutral drift within a broad definition of the aposematic signal defined by potential predators. Aposematic patterning, therefore, appears to be a highly complex adaptation, combining different processes at different spatial scales and in different contexts. Future research is needed to understand how these multiple selection pressures interact across wider temporal and spatial dimensions.

Methods

Study site and image collection. Experiments took place in the rainforest surrounding the Saut Pararé camp of La Station de Recherche en Écologie des Nouragues, French Guiana, between December 2014 and January 2015. We photographed adult *D. tinctorius* on their natural leaf litter background at a height of 70 cm (n = 84), as well as the leaf litter without frogs at 100 cm (n = 265) and 150 cm (n = 265). *In situ* photographs were taken with a Nikon D3200 DSLR and AF-S DX NIKKOR 35 mm lens (Nikon Corporation, Tokyo, Japan) and contained a ColorChecker Passport (X-Rite Inc. 2009. MI, USA). *Ex situ* UV photographs were taken of captive *D. tinctorius* and the plasticine models, using a Nikon D70 DSLR (Nikon Corporation, Tokyo, Japan) and UV-VIS 105 mm CoastalOpt® SLR lens (Jenoptik AG, Jena, Germany) with human-visible and IR blocking filters, and each image contained a 15% reflectance Spectralon® grey standard (Labsphere, Inc. North Sutton, NH, USA).

Visual modeling. Photographs of the frogs on their natural background (n = 84) were calibrated and scaled using the ColorChecker Passport (57), and 1000 pixels from the frog and 1000 pixels from the background were randomly selected for analysis. We used five different visual models: tetrachromatic avian, both VS (*Pavo cristatus* (58)) and UV (*Sturnus vulgaris* (59)) sensitive, trichromatic snake (*Masticopis flagellum* (60)), dichromatic mammal (*Mustela putorius* (61)), and trichromatic human (62). As opponent processing is central to human color perception (63), and evidence suggests a similar

mechanism for avian color perception (64-66), each visual model used relative cone capture rates to generate a three-dimensional color space made up of Luminance (L) and the opponent channels red-green (rg), and yellow-blue (yb) (19, 20, 67). All visual modeling was performed in MATLAB 2015a (The MathWorks Inc. Natick, MA, USA).

To represent increasing viewing distance, we used a log-Gabor filter bank with four spatial scales (wavelength relative to the smallest frog: Very high = ⅛, High = ¼, Medium = ½, and Low = 1) and six orientations (0º - 150º in 30º increments) (41, 68, 69). To assess discriminability between frog and background at each spatial scale we used Support Vector Machines (SVMs: R package *e1071* (37)) in R 3.1.3 (The R Foundation for Statistical Computing, Vienna, Austria). SVMs act as a non-linear classifier, projecting the data into a multi-dimensional space in which a hyperplane can be fitted between groups (39). Data were cross-validated by training the model on one half of the data and testing on the other (39). Classification accuracy was assessed using the Area Under the Curve (AUC) of Receiver Operated Characteristic (ROC) curves (R package *pROC* (38)) in R 3.1.3. See *Supporting Methods* and (19, 20, 41, 67).

Survival. We used plasticine model frogs to record avian predation *in situ*. Plasticine frogs were designed to represent the natural pattern (N – yellow-and-black), aposematism (Y – plain yellow), and camouflage (C – brown-and-black). Model frogs were presented on four backgrounds: the natural leaf litter (NL), a paper square printed with leaf litter (PL), and two manipulated backgrounds which differed from the natural substrate, natural soil (NS) and a homogeneously colored paper square (PA). This created 12 treatments (frog-background pairs).

A randomized block design was used. Twelve blocks containing seven of each treatment (n = 1008: 84 per treatment) were placed along non-linear transects through the rainforest. Stimuli were inspected for signs of avian predation at 24, 48, 72, and 96 hours. Predation risk was analyzed with a mixed-effects Cox model (R package *coxme* (70)) in R 3.1.3. Avian predation was included as a full event, whereas non-

avian predation, missing or washed out stimuli, and those surviving to 96 h were included as censored values, and block was included as a random factor. See *Supporting Methods*.

Detection. Photographs of 30 different *D. tinctorius* were randomly selected and the colors of each frog were manipulated to create 12 different treatments (n = 360). To allow for pattern manipulation the colors of each frog were standardized using *k*-means clustering. The RGB color space was grouped into four clusters, with the centroid with the highest ratio of R+G to B designated yellow, and that with the lowest luminance designated black. These manipulations created 12 treatments: A - natural pattern using standardized colors, B - plain blue-black, C - plain yellow, D - reversed color natural pattern, E - all yellow pixels of A grouped into one approximately circular patch, F - all yellow pixels from A moved to the frog's edge, G - natural pattern with yellow replaced with the mean color of the background, H - inverse of pattern G, I - mean color of the frog, J: mean color of the background, K - background matching camouflage (random sample of leaf litter background), and L: unmanipulated natural frog pattern (Fig. S6).

Three different viewing distances were created using calibrated photographs of leaf litter taken at different distances (100 cm = 265, 150 cm = 265). Each frog was appropriately scaled and randomly placed onto the leaf litter (as the number of frogs (360) outnumbered the number of backgrounds (265), 95 background images were randomly selected and rotated by 90º). The 100 cm images created the Near condition and the 150 cm images created the Medium distance. The Far condition was generated by reassigning the frogs to the 150 cm images and applying a 16º Gaussian filter to remove high spatial frequency information.

Human participants (n = 18) searched for frogs on a computer screen. The stimuli were presented to each participant in three sessions (each distance as a separate session), each of which contained all 360 stimuli, split into 10 blocks of 36 images, in an individually randomized sequence (n = 540 per frog-distance

303 combination). We recorded reaction time and detection probability in *Psychtoolbox* (71) in MATLAB
304 2015a. All participants gave their informed consent in line with the Declaration of Helsinki.

305 Detection probability was analyzed with a binomial generalized mixed effects model and log-transformed
306 reaction time analyzed with a general linear mixed effects model (R package *lme4* (72)) in R 3.1.3. Both
307 models included treatment and distance as fixed effects, and participant number as a random factor.
308 Pairwise comparisons of a priori interest were calculated (R package *multcomp* (73)) to test three
309 hypotheses: whether the natural pattern is organized to act as i) maximal conspicuousness, ii) disruptive
310 camouflage, and iii) distance-dependent pattern blending. See *Supporting Methods*.

Acknowledgments. We thank all CNRS staff for their help in and out of the field, and Bibiana Rojas (University of Jyväskylä) for sharing her knowledge of the opportunities at Nouragues and for discussion. We thank Bristol Zoo Gardens (Bristol Zoological Society), The Living Rainforest (The Trust for Sustainable Living), and Dartfrog (www.dartfrog.co.uk) for access to *ex situ* tropical environments and frogs. We also thank three anonymous reviewers for their very helpful comments. This work was supported by the Centre National de la Recherche Scientifique, France (ANR-10-LABX-25-01 to all authors) and the Biotechnology & Biological Sciences Research Council, UK: (BB/N007239/1 to ICC). J.B.B. was supported by a University of Bristol Postgraduate Scholarship. I.C.C. thanks the Wissenschaftskolleg zu Berlin for support during part of the study.

Author contributions: J.B.B., N.E.S-S., and I.C.C. conceived the study. J.B.B. and C.M. collected the images and performed the survival experiment in the field, J.B.B. collected *ex situ* photographic data and ran the visual search experiment, and I.C.C. wrote the programs for the latter and image analysis. All authors contributed to the design and interpretation of experiments. J.B.B. wrote the first draft of the manuscript, with subsequent modifications by all authors.

The authors declare no conflict of interest.

References

1 Saporito RA, Donnelly MA, Spande TF, Garraffo HM (2012) A review of chemical ecology in poison frogs. *Chemoecology* 22:159-168.

2 Rojas B (2017) Behavioural, ecological, and evolutionary aspects of diversity in frog colour patterns. *Biol. Rev.* 92:1059-1080.

3 Gamberale-Stille G (2001) Benefit by contrast: an experiment with live aposematic prey. *Behav. Ecol.* 12:768-772.

4 Kenward B, Wachtmeister C-A, Ghirlanda S, Enquist M (2004) Spots and stripes: the evolution of repetition in visual signal form. *J. Theor. Biol*. 230:407-419.

5 Aronsson M, Gamberale-Stille G (2013) Evidence of signaling benefits to contrasting internal color boundaries in warning coloration. *Behav. Ecol.* 24:349-354.

6 Barnett C, Bateson M, Rowe C (2007) State-dependent decision making: educated predators strategically trade off the costs and benefits of consuming aposematic prey. *Behav. Ecol.* 18:645-651.

7 Skelhorn J, Rowe C (2007) Predators' toxic burdens influence their strategic decisions to eat toxic prey. *Curr. Biol.* 17:1479-1483.

8 Barnett CA, Skelhorn J, Bateson M, Rowe C (2012) Educated predators make strategic decisions to eat defended prey according to their toxin content. *Behav. Ecol.* 23:418-424.

9 Chatelain M, Halpin CH, Rowe C (2013) Ambient temperature influences birds' decisions to eat toxic prey. *Anim. Behav.* 86:733-740.

10 Halpin C, Skelhorn J, Rowe C (2014) Increased predation of nutrient-enriched aposematic prey. *Proc. R. Soc. B.* 281:20133255.

11 Myers CW, Daly JW, Malkin B (1978) A dangerously toxic new frog (*Phyllobates*) used by Emberá Indians of Western Colombia, with discussion of blowgun fabrication and dart poisoning. *Bull. Am. Mus. Nat. His.* 161:311-365.

12 Master TL (1999) Predation by rufous motmot on black and green poison frog. *Wilson Bull.* 111:439-440.

13 Alvarado JB, Alvarez A, Saporito RA (2013) *Oophaga pumilio* (strawberry poison frog): predation. *Herpetol. Rev.* 44:298.

14 Endler JA (1978) A predator's view of animal color patterns. *Evol. Biol.* 11:319-364.

15 Bohlin T, Tullberg BS, Merilaita S (2008) The effect of signal appearance and distance on detection risk in an aposematic butterfly larva (*Parnassius apollo*). *Anim. Behav.* 76:577-584.

16 Tullberg BS, Merilaita S, Wiklund C (2005) Aposematism and crypsis combined as a result of distance dependence: functional versatility of the colour pattern in the swallowtail butterfly larva. *Proc. R. Soc. B.* 272:1315-1321.

17 Caro T, Stankowich T, Kiffner C, Hunter J (2013) Are spotted skunks conspicuous or cryptic? *Ethol. Ecol. Evol.* 25:144-160.

18 Barnett JB, Cuthill IC (2014) Distance-dependent defensive coloration. *Curr. Biol.* 24:R1157-R1158.

19 Barnett JB, Cuthill IC, Scott-Samuel NE (2017) Distance-dependent pattern blending can camouflage salient aposematic signals. *Proc. R. Soc. B.* 284:20170128.

20 Barnett JB, Scott-Samuel NE, Cuthill IC (2016) Aposematism: balancing salience and camouflage. *Biol. Lett.* 12:20160335.

21 Stevens M (2007) Predator perception and the interrelation between different forms of protective coloration. *Proc. R. Soc. B.* 274:1457-1464.

370 22 Endler JA, Mappes J (2004) Predator mixes and the conspicuousness of aposematic signals. *Am. Nat*.
371 163:532-547.

372 23 Summers K, Speed MP, Blount JD, Stuckert AMM (2015) Are aposematic signals honest? A review.
373 *J. Evol. Biol*. 28:1583-1599.

374 24 Honma A, Mappes J, Valkonen JK (2015) Warning coloration can be disruptive: aposematic marginal
375 wing patterning in the wood tiger moth. *Ecol. Evol*. 5:4863-4874.

376 25 Stevens M, Merilaita S (2009) Defining disruptive coloration and distinguishing its functions. *Philos.*
377 *Trans. R. Soc. B.* 364:481-488.

378 26 Stevens M, Cuthill IC, Windsor AMM, Walker HJ (2006) Disruptive contrast in animal camouflage.
379 *Proc. R. Soc. B.* 273:2433-2438.

380 27 Prudic KL, Skemp AK, Papaj DR (2007) Aposematic coloration, luminance contrast, and the benefits
381 of conspicuousness. *Behav. Ecol*. 18:41-46.

382 28 Schaefer HM, Stobbe N (2006) Disruptive coloration provides camouflage independent of
383 background matching. *Proc. R. Soc. B.* 273:2427-2432.

384 29 Forsman A, Merilaita S (1999) Fearful symmetry: pattern size and asymmetry affects aposematic
385 signal efficacy. *Evol. Ecol.* 13:131-140.

386 30 Cuthill IC, Stevens M, Windsor AMM, Walker HJ (2006) The effects of pattern symmetry on
387 detection of disruptive and background-matching coloration. *Behav. Ecol.* 17:828-832.

388 31 Karpestam E, Merilaita S, Forsman A (2014) Natural levels of colour polymorphism reduce
389 performance of visual predators searching for camouflaged prey. *Biol. J. Linn. Soc.* 112(3):546-555.

390 32 Marshall NJ (2000) Communication and camouflage with the same 'bright' colours in reef fishes.
391 *Philos. Trans. R. Soc. B.* 355:1243-1248.

33 Barnett JB, et al. (2017) Stripes for warning and stripes for hiding: spatial frequency and detection distance. *Behav. Ecol.* 28:373-381.

34 Rojas B, Endler JA (2013) Sexual dimorphism and intra-populational colour pattern variation in the aposematic frog Dendrobates tinctorius. *Evol. Ecol.* 27:739-753.

35 Rojas B, Rautiala P, Mappes J (2014) Differential detectability of polymorphic warning signals under varying light environments. *Behav. Process*. 109:164-172.

36 Willink B, García-Rodríguez A, Bolaños F, Pröhl H (2014) The interplay between multiple predators and prey colour divergence. *Biol. J. Linn. Soc.* 113:580-589.

37 Meyer D, Dimitriadou E, Hornik K, Weingessel A, Leisch F (2017) e1071: Misc Functions of the Department of Statistics, Probability Theory Group (Formerly: E1071), TU Wien. R package version 1.6-8. https://cran.r-project.org/package=e1071.

38 Robin X, et al. (2011) pROC: an open-source package for R and S+ to analyze and compare ROC curves. *BMC Bioinformatics* 12:77.

39 Lantz B (2013) Machine learning with R (Packt Publishing Ltd., Birmingham, UK).

40 Barnett JB, Michalis C, Scott-Samuel NE, Cuthill IC (2017) Data from "Distance-dependent defensive coloration in the poison frog *Dendrobates tinctorius*, Dendrobatidae". University of Bristol Research Data Repository. doi to be added.

41 Michalis C, Scott-Samuel NE, Gibson DP, Cuthill IC (2017) Optimal background matching camouflage. *Proc. R. Soc. B.* 284:20170709.

42 Merilaita S, Tullberg BS (2005) Constrained camouflage facilitates the evolution of conspicuous warning coloration. *Evolution* 59:38-45.

413 43 Comeault AA, Noonan BP (2011) Spatial variation in the fitness of divergent aposematic phenotypes
414 of the poison frog, *Dendrobates tinctorius*. *J. Evol. Biol.* 24:1374-1379.

415 44 Noonan BP, Comeault AA (2009) The role of predator selection on polymorphic aposematic poison
416 frogs. *Biol. Lett*. 5:51-54.

417 45 Gamberale-Stille G, Tullberg BS (1999) Experienced chicks show biased avoidance of stronger
418 signals: an experiment with natural colour variation in live aposematic prey. *Evol. Ecol.* 13:579-589.

419 46 Stevens M, Ruxton GD (2012) Linking the evolution and form of warning coloration in nature. *Proc.*
420 *R. Soc. B.* 279:417-426.

421 47 Maan ME, Cummings ME (2009) Sexual dimorphism and directional sexual selection on aposematic
422 signals in a poison frog. *PNAS* 106:19072-19077.

423 48 Maan ME, Cummings ME (2008) Female preferences for aposematic signal components in a
424 polymorphic poison frog. *Evolution* 62:2334-2345.

425 49 Rojas B, Devillechabrolle J, Endler JA (2014) Paradox lost: variable colour-pattern geometry is
426 associated with differences in movement in aposematic frogs. *Biol. Lett.* 10:20140193.

427 50 Hämäläinen L, Valkonen J, Mappes J, Rojas B (2015) Visual illusions in predator–prey interactions:
428 birds find moving patterned prey harder to catch. *Animal Cogn*. 18:1059-1068.

429 51 Mappes J, Kokko H, Ojala K, Lindström L (2014) Seasonal changes in predator community switch
430 the direction of selection for prey defences. *Nat. Commun*. 5:5016.

431 52 Saporito RA, Donnelly MA, Garraffo HM, Spande TF, Daly JW (2006) Geographic and seasonal
432 variation in alkaloid-based chemical defenses of *Dendrobates pumilio* from Bocas del Toro, Panama.
433 *J. Chem. Ecol.* 32:795-814.

53 Daly JW, et al. (2002) Bioactive alkaloids of frog skin: Combinatorial bioprospecting reveals that pumiliotoxins have an arthropod source. *PNAS* 99:13996-14001.

54 Born M, Bongers F, Poelman E, Sterck F (2010) Dry-season retreat and dietary shift of the dart-poison frog *Dendrobates tinctorius* (Anura: Dendrobatidae). *Phyllomedusa* 9:37-52.

55 Wollenberg KC, Lötters S, Mora-Ferrer C, Veith M (2008) Disentangling composite colour patterns in a poison frog species. *Biol. J. Linn. Soc*. 93:433-444.

56 Wollenberg KC, Veith M, Noonan BP, Lötters S (2006) Polymorphism versus species richness: systematics of large *Dendrobates* from the eastern Guiana Shield (Amphibia: Dendrobatidae). *Copeia* 2006:623-629.

57 Stevens M, Párraga CA, Cuthill IC, Partridge JC, Troscianko TS (2007) Using digital photography to study animal coloration. *Biol. J. Linn. Soc.* 90: 211-237.

58 Hart NS (2002) Vision in the peafowl (Aves: *Pavo cristatus*). *J. Exp. Biol.* 205:3925-3935.

59 Hart NS, Partridge JC, Cuthill IC (1998) Visual pigments, oil droplets and cone photoreceptor distribution in the European starling (*Sturnus vulgaris*). *J. Exp. Biol.* 201:1433-1446.

60 Macedonia JM, et al. (2009) Conspicuousness of Dickerson's collared lizard (*Crotaphytus dickersonae*) through the eyes of conspecifics and predators. *Biol. J. Linn. Soc*. 97:749-765.

61 Calderone JB, Jacobs GH (2003) Spectral properties and retinal distribution of ferret cones. *Vis. Neurosci*. 20:11-17.

62 Smith VC, Pokorny J (1975) Spectral sensitivity of the foveal cone photopigments between 400 and 500 nm. *Vision Res.* 15:161-171.

63 Hurvich LM, Jameson D (1957) An opponent-process theory of colour vision. *Psychol. Rev*. 64:384-404.

64 Kelber A (2016) Colour in the eye of the beholder: receptor sensitivities and neural circuits underlying colour opponency and colour perception. *Curr. Opin. Neurobiol*. 41:106-112.

65 Vorobyev M, Osorio D (1998) Receptor noise as a determinant of colour thresholds. *Proc. R. Soc. B.* 265:351-358.

66 Goldsmith TH, Butler BK (2005) Color vision of the budgerigar (*Melopsittacus undulatus*): hue matches, tetrachromacy, and intensity discrimination. *J. Comp. Physiol. A* 191:933-951.

67 Xiao F, Cuthill IC (2016) Background complexity and the detectability of camouflaged targets by birds and humans. *Proc. R. Soc. B.* 283:20161527.

68 Field DJ (1987) Relations between the statistics of natural images and the response properties of cortical cells. *J. Opt. Soc. Am. A.* 4:2379-2394.

69 Gabor D (1946) Theory of communication. *J. I. Electr. Eng*. 93:429-441.

70 Therneau TM (2015) coxme: mixed effects cox models. R package version 2.2-5. http://cran.r-project.org/package=coxme.

71 Brainard DH (1997) The psychophysics toolbox. *Spat. Vis*. 10:433-436.

72 Bates D, Maechler M, Bolker B, Walker S (2015) lme4: linear mixed-effects models using Eigen and S4. R package version 1.1-9. http://cran.r-project.org/package=lme4.

73 Hothorn T, Bretz F, Westfall P (2008) Simultaneous inference in general parametric models. *Biom. J.* 50:346-363.

Figures

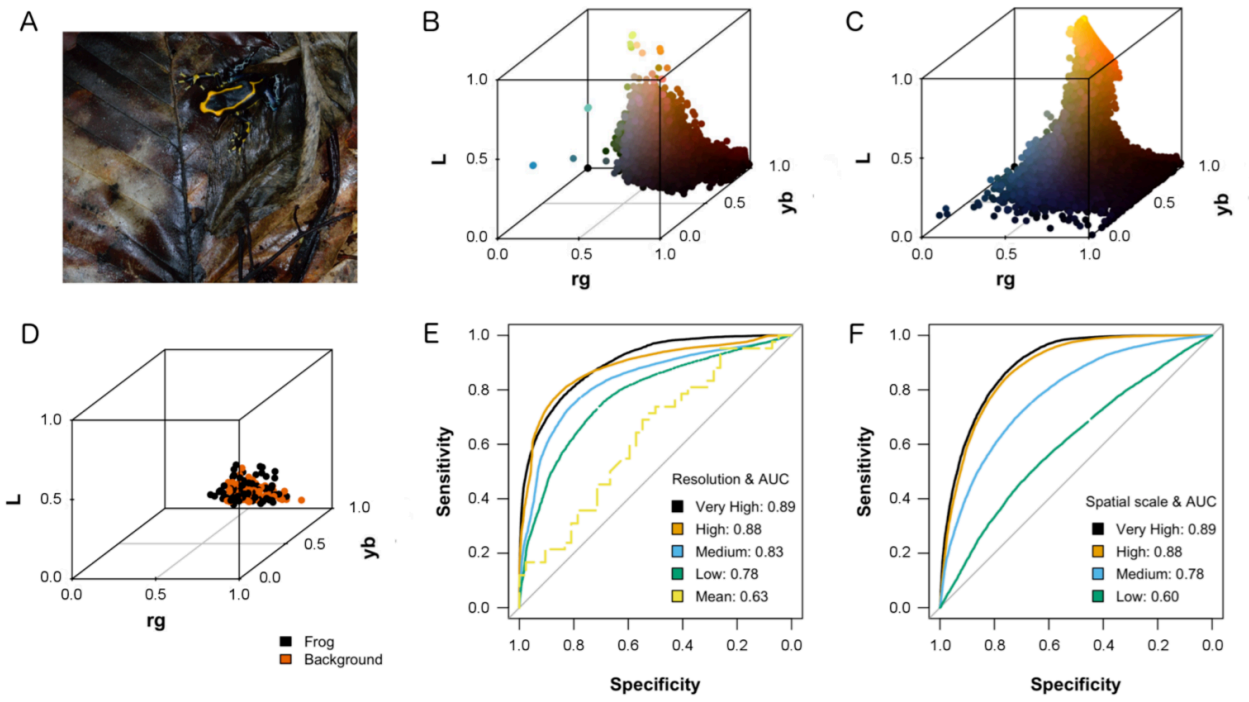

Fig. 1. Avian (VS) visual modeling of *D. tinctorius* and the leaf litter background (n = 84), the trends are consistent with the other four visual models (see *Supplementary Figures*). At close-range *D. tinctorius* and its background are easily discriminated, but at greater viewing distances classification accuracy declines. A: *D. tinctorius* photographed *in situ*. B: leaf litter colors in avian visual space. C: *D. tinctorius* coloration in avian visual space - the frog contains high luminance yellows and low luminance blue-blacks which are not found in the background. D: the mean colors of each frog and each background sample are intermixed. E: color discrimination (ROC curves) at different spatial resolutions - as resolution decreases (increasing distance), accuracy decreases. F: texture discrimination (ROC curves) at different spatial scales - as resolution decreases, accuracy decreases.

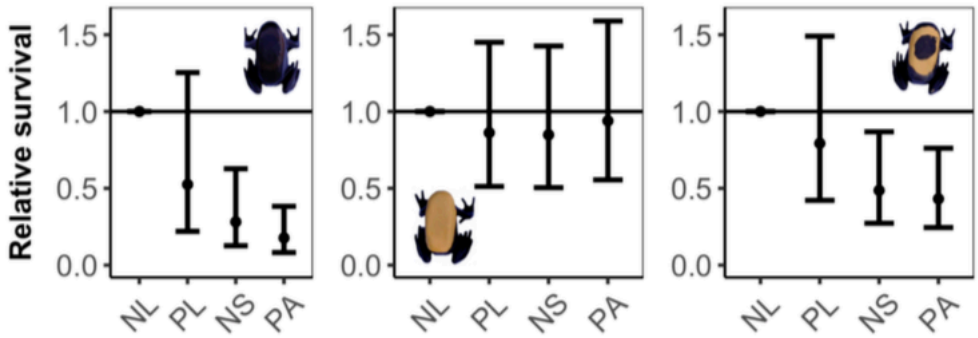

485

486 **Fig. 2.** Relative survival of plasticine frogs in comparison to the natural leaf litter background (NL). Odds
487 ratios with 95% confidence intervals from the model (n = 84 per frog-background combination). Left
488 (cryptic brown-and-black frogs (C)): there was no significant difference between the natural background
489 (NL) and the printed leaf litter (PL), but there was a significantly lower survival for the modified (NS and
490 PA) backgrounds. Middle (plain yellow frogs (Y)): there was no significant effect of changing
491 background. Right (yellow-and-black frogs (N)): there was no significant difference between NL and PL,
492 but NL had a significantly higher survival than both NS and PA. The survival of the natural yellow-and-
493 black pattern was dependent on the visual characteristics of the background, suggesting a camouflage
494 component.

495

496

497

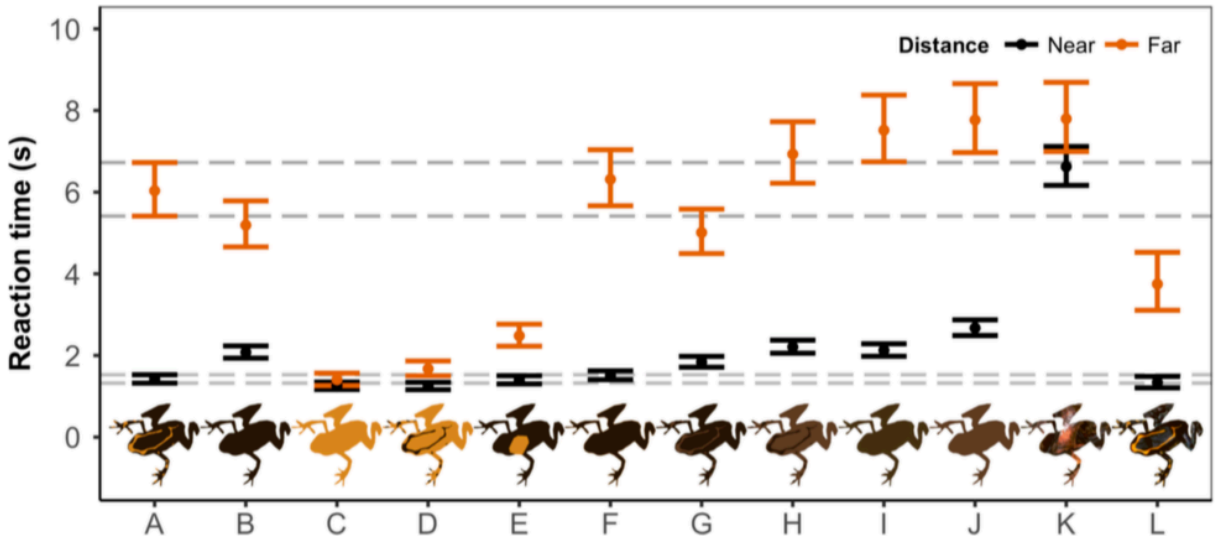

498

499 **Fig. 3.** Time taken by human observers to detect frogs at the Near and Far distances. Means with 95%
500 confidence intervals from the model (n = 540 per frog-distance combination): grey lines indicate 95% CI
501 for treatment A (posterized natural pattern). At close-range (Near - black) the natural phenotype (A)
502 groups readily with conspicuous (high yellow) patterns (C, D, and E), which are detected more quickly
503 than cryptic patterns (B, F, G, H, I, J, and K). At the greatest distance (Far – orange) the natural
504 phenotype is detected significantly more slowly than conspicuous patterns, and groups more readily with
505 cryptic patterns.

506

Supporting Methods

Study site. Image collection and the survival experiment took place at the Saut Pararé camp of La Station de Recherche en Écologie des Nouragues (The Nouragues Ecological Research Station), Nouragues Natural Reserve, French Guiana (4˚02'N 52˚41'W). The site is an uninhabited area of primary tropical rainforest with the year split into wet (December-July) and dry (August-November) seasons (1). Field experiments were conducted between December 2014 and January 2015 at the beginning of the wet season.

Image collection. Captive *Dendrobates tinctorius* (n = 3) were photographed with a UV-sensitive Nikon D70 Digital SLR camera (Nikon Corporation, Tokyo, Japan) and UV-VIS 105 mm CoastalOpt® SLR lens (Jenoptik AG, Jena, Germany) plus human-visible and IR blocking filters. Frogs were illuminated by a 13W Exo Terra Full Spectrum Daylight bulb (PT2190, Exo Terra (Hagen Inc.), Montréal, Canada) and the images contained a 15% reflectance Spectralon® grey standard (Labsphere, Inc. North Sutton, NH, USA) to allow standardization of reflectance values between VIS and UV photographs. This was repeated for the frog-like stimuli used in the survival experiment. This revealed minimal UV reflectance from both the real frogs and frog-like stimuli.

Wild adult *D. tinctorius* were searched for along approximately linear transects through the rainforest surrounding the Saut Pararé camp. Once detected, frogs (n = 84) were photographed with a Nikon D3200 Digital SLR camera and AF-S DX NIKKOR 35 mm prime lens (Nikon Corporation, Tokyo, Japan). Frogs were photographed against their natural leaf litter background from directly above at a height of 70 cm. All images contained a ColorChecker Passport (X-Rite Inc. 2009. MI, USA) which allowed color calibration and appropriate scaling. Additional photographs of the leaf litter, without frogs, were taken from directly above at heights of 100 cm (n = 265) and 150 cm (n = 265).

This was repeated for the survival experiment: the plasticine frog-like stimuli were photographed on their experimental backgrounds from a height of 100 cm (n = 58: 5 of each of the 12 frog-background

combinations – two images, one CNL and one NPL were excluded from the analysis due to dirt on the ColorChecker). Frogs were separated from their backgrounds in MATLAB 2015a (The MathWorks Inc. Natick, MA, USA) and the colors of each were plotted in the color space generated from the VS avian visual model (C = 14, Y = 15, N = 14, NL = 19, PL = 19, NS = 20, and PA = 20). This revealed that the brown-and-black frog closely matched the natural background (NL), but not the modified background (PA), whereas the yellow component of the plain yellow (Y) and natural pattern (N) frogs was distinct from all backgrounds (Fig. S5).

Visual modelling. Five visual systems were used: human LMS, violet-sensitive (VS) avian LMS, UV-sensitive (UV) avian LMS, snake LMS, and carnivorous mammal LS. Human vision was included to allow intuitive interpretation of results. In humans, opponent processing is key to our understanding of color perception (2), and central to the international standard color space L*a*b*. L*a*b* color space was derived from psychophysical testing and splits color into a measure of luminance (L*) and the opponent channels, red-green (a*) and yellow-blue (b*) (CIELAB, 1976). However, as an equivalent color space is not available for nonhuman species, and there is evidence of opponent processing in birds (3-5), we used the opponent channel logic of L*a*b* to generate visual models from relative cone capture rates (6-8).

Human LMS was produced from the trichromatic human visual pigments with peak absorption (λ_{max}) at 564 nm (L), 534 nm (M), and 420 nm (S) (9). Carnivorous mammal LS followed the dichromatic vision of the domestic ferret (*Mustela putorius* Mustelidae) with λ_{max} at 558 nm (L) and 430 nm (S) (10), and snake LMS followed the trichromatic UV-sensitive vision of the whip snake (*Masticophis flagellum* Colubridae) with λ_{max} at 561 nm (L), 458 nm (M), and 362 nm (UV) (11).

The violet-sensitive (VS) avian LMS model followed the tetrachromatic vision of the Indian peafowl (*Pavo cristatus* Galliformes) with λ_{max} at 605 nm (L), 537 nm (M), 477 nm (S), 432 nm (VS), and luminance measuring double cones at 567 nm (D) (12). The UV-sensitive avian LMS model used the

554 European starling (*Sturnus vulgaris* Passeriformes) with λ_{max} of 563 nm (L), 504 nm (M), 449 nm (S), 362
555 nm (UV), and 563 nm (D) (13).

556 Dendrobatid frogs (*Dendrobates*, *Phyllobates*, and *Oophaga* spp.) and clay models representing
557 dendrobatid species, have been observed falling prey to birds (both UV (14, 15) and VS (16) sensitive
558 (17, 18)) and snakes (19). Although the visual models do not correspond directly to sympatric predatory
559 species of *D. tinctorius*, visual perception is largely conserved among carnivorous mammals (20) and
560 although birds fall into two categories (UV or VS sensitive) variation within each category is minimal
561 (17). Our models are, therefore, representative of many predatory mammals and birds. Snake vision, on
562 the other hand, is highly variable (21). However, as no data exist for the most ecologically relevant
563 species, we follow previous studies on how snakes may perceive dendrobatid frog coloration (22, 23).

564 To assess how well the camera (Nikon D3200, Nikon Corporation, Tokyo, Japan) could recreate the
565 wavelength sensitivity of the visual models, we compared the response of each receptor pigment to the
566 nearest camera sensor (UV, VS, and S cones to the blue (B) sensor, the M cone to the green (G) sensor,
567 and the L and D cones to the red (R) sensor), when viewing 18900 spectral measurements of temperate
568 vegetative scenes. This revealed a high correlation between the camera and all visual pigments ($R^2 > 0.95$,
569 except for avian and snake UV cones to the B sensor where $R^2 = 0.69$).

570 Human LMS was modelled in 3-dimensional color space. Luminance was the mean of the combined L
571 and M cone responses (24), the red-green opponent channel (rg) was the relative photon catch between
572 the L and M cones (ratio of L-M to L+M), and the yellow-blue opponent channel (yb) was the ratio of the
573 combined L and M channels to the S cone (ratio of (M+L-2*S) to (M+L+S)). The dichromatic mammal
574 lacks an M channel and so luminance was measured from the L cone (24), and yb from the ratio of L to S
575 cones (ratio of (L-S) to (L+S)).

576 As there was minimal UV reflectance from the frog, a high correlation between both the VS and S cones
577 to the B sensor, and UV light is largely filtered out beneath the canopy of tropical rainforest (25), both

avian LMS models were calculated in the same way as human LMS (luminance, rg, and yb channels) but with luminance measured from the response of the D cone (24). However, due to uncertainties regarding UV reflectance, including potential differences between captive and wild populations, we focus on the VS avian model (Fig. 1). For snake LMS luminance was measured from the L cone, rg from the relative stimulation of L to M cones (ratio of (L-M) to (L+M)) and yb from the relative stimulation of the combined L and M cones to the UV cone (ratio of (M+L-2*UV) to (M+L+UV)). See (6) and (8) for further discussion.

All visual systems were used for *D. tinctorius* (n = 84), whereas as UV reflectance was minimal, and as we only recorded avian predation, we only used the VS avian model in the survival experiment. All visual modeling was performed in MATLAB 2015a.

Image analysis. From each calibrated image of *D. tinctorius* (n = 84) 1000 pixels from the leaf litter and 1000 pixels from the frog were randomly selected, without replacement, for analysis using MATLAB's random number generator for a discrete uniform distribution. Missing values due to saturation (n = 11 pixels) were replaced using *k*-nearest-neighbors data imputation (R package *DMwR* (26)) in R 3.1.3 (The R Foundation for Statistical Computing, Vienna, Austria).

A log-Gabor filter bank with four spatial scales (wavelengths expressed relative to the smallest frog: Very high = ⅛, High = ¼, Medium = ½, and Low = 1), and six orientations (0˚ - 150˚ in 30˚ increments) was used to assess visual texture (27-29). We do not specify a particular distance as visual acuity and contrast sensitivity depend on light intensity, which will change continuously in the field. These filters, instead, ensure that we can simulate how the pattern would be perceived at distances above and below the resolution limit of the pattern without obscuring the whole frog.

Support Vector Machines (SVMs) were used to assess how easily frogs and backgrounds could be discriminated at different spatial scales (R package *e1071* (30)). SVMs were used because the yellow and blue colors of the frog fall on either side of the background color distributions and so a classifier with a

single decision boundary (e.g. logistic regression) would not be effective. To avoid overfitting, cross-validation was implemented by randomly splitting the data in two, training the model on one half and testing the model on the other (31). Classification accuracy was assessed using the area under the curve (AUC) of receiver operating characteristic (ROC) curves (R package *pROC* (32)). Plotting the proportion of correct frog classifications (sensitivity) against the proportion of correct background classifications (specificity), with the x-axis reversed, presents increasing accuracy towards the top-left of the panel. An AUC of 1.0 equates to perfect classification whereas 0.5 equals random chance, and the AUC was interpreted as: 1.0-0.9 = excellent, 0.9-0.8 = good, 0.8-0.7 = fair, 0.7-0.6 = poor, 0.6-0.5 = fail (31).

Survival experiment. In order to assess whether the survival of *D. tinctorius* is background dependent (a feature of camouflage rather than aposematism (29, 33)) we used plasticine model frogs, manipulated both the frog's color and the background, and recorded the rate of avian predation *in situ*.

Frog-like stimuli consisted of a reusable plastic base (legs) and a soft plasticine top (head and body) in which predation marks could be identified. To form the base, commercially available plastic models of *D. tinctorius* (n = 200; Blip LLC. Plymouth, MN, USA) were cut along the frontal plane. To form the head and body of the frog white non-toxic plasticine (Newplast^{TM}, Newclay Products Ltd. Newton Abbott, UK) was cut into ~5 g blocks and molded by hand. Our stimuli were ~45 mm in length, which fell within the 37-53 mm length range previously recorded for this population of *D. tinctorius* (34).

All plastic bases were painted black (Carbon Black Liquitex Professional, ColArt Interactive Inc. Piscataway, NJ, USA), and the plasticine tops were painted either yellow (n = 800; Cadmium Yellow Deep Hue 5 Liquitex Professional, ColArt Interactive Inc. Piscataway, NJ, USA) or brown (n = 400; Raw Umber Liquitex Professional, ColArt Interactive Inc. Piscataway, NJ, USA). A roughly circular black pattern was then stenciled by hand onto half of the yellow (n = 400) and all of the brown (n = 400) frogs. This created 400 of each treatment: plain yellow (^{Y}), brown-and-black (^{C}), and yellow-and-black (^{N}).

625 The model frogs were then placed onto one of four experimental backgrounds with different visual
626 characteristics (Figs. S4 and S5). Two backgrounds were created *in situ*: NL – the natural leaf litter
627 covering the rainforest floor on which frogs are predominantly active, and NS – the plain soil found
628 beneath the leaf litter. The other two backgrounds were generated *ex situ* from photographs of rainforest-
629 like leaf litter found in the tropical house exhibits of Bristol Zoo Gardens (Bristol Zoological Society,
630 Bristol, UK) and The Living Rainforest (The Trust for Sustainable Living, Berkshire, UK). PL was a leaf
631 litter photograph and PA was the mean RGB color and luminance of the leaf litter photograph calculated
632 in ImageJ (National Institutes of Health, MD, USA). Both PL and PA were calibrated to produce a 1:1
633 scale and appropriate colors and were then printed at 120 dpi (Canon imageRunner Advance C5235i,
634 Canon Inc. Tokyo, Japan) on to 100 mm^2 sheets of waterproof paper (Rite-in-the-Rain White All-Weather
635 Copier Paper 8512-M, JL Darling LLC. Tacoma, WA, USA).

636 A randomized block design was used. Twelve blocks of plasticine frogs (n = 1008: seven replicates of
637 each of the 12 treatments per block) were independently placed along non-linear transects through the
638 rainforest, the route and length of each transect varied following local terrain. For each block, the frog-
639 background pairs were placed onto the leaf litter in a random sequence (decided by coin toss *in situ*) and
640 were positioned in order to be unobstructed by vegetation and to be independent (out of sight) from one
641 another, such that it would be unlikely for any one predator to encounter more than one model at a time.

642 The occurrence of avian predation was recorded at 24, 48, 72, and 96 h after the block was set up. Avian
643 predation was identified by clear beak marks in the plasticine, whereas other forms of predation were
644 identified by visible tooth marks (mammals and reptiles) or small pits (ants). The rate of predation was
645 analyzed using a mixed-effects Cox model (R package *coxme* (35)) in R 3.1.3. Avian predation was
646 included as a full event, whereas non-avian predation, missing or washed out stimuli, and those surviving
647 to 96 h were included as censored values, and block was included as a random factor.

Detection experiment. Experimental stimuli were based on photographs of *D. tinctorius* and its natural leaf litter background (see above). Photographs of 30 different *D. tinctorius* were randomly selected and, after color calibration and scaling, each was cropped from the image and saved separately. Each frog photograph was then manipulated into 12 different color treatments in MATLAB 2015a (Fig. S6).

To allow manipulation of color patterning we generated standardized colors using *k*-means clustering of each *D. tinctorius*. The colors of each frog were grouped into four clusters, and we designated the 'yellowest' centroid (highest ratio of R+G to B) as yellow, and the lowest luminance centroid as blue-black. Each frog generated slightly different colors, and these standardized colors were used to generate treatments A, B, C, D, E, and F.

Treatment A recreated the natural pattern (predominantly blue-black with a yellow pattern) with standardized yellow and blue-black colors. Treatment B was homogeneous blue-black and treatment C was homogeneous yellow. For treatment D, we reversed the yellow and blue-black regions of treatment A (creating a predominantly yellow frog with blue-black patterning). For treatment E, all yellow pixels found in treatment A were grouped together to form an approximately circular patch of yellow on an otherwise blue-black frog, and in treatment F, all yellow pixels found in treatment A were layered around the frog's edge.

To create treatment G all yellow pixels of treatment A were replaced with the average color of the background, creating a predominantly black frog with a brown pattern, and these regions were reversed for treatment H (predominantly brown with a black pattern). Treatment I and treatment J were homogeneous brown: the average colors of the frog and of the background respectively. Treatment K represented background matching camouflage and was a randomly selected frog shaped patch of leaf litter cropped from an appropriately scaled and calibrated photograph of French Guianan leaf litter. Finally, treatment L was the unmanipulated frog.

671 These manipulations were performed on each replicate *D. tinctorius* separately to create 30 replicates of
672 12 different treatments (n = 360).

673 Three different backgrounds were generated, to represent three different viewing distances, from
674 photographs of leaf litter taken in French Guiana. Each image (100 cm = 265; 150 cm = 265) was
675 converted to an 8-bit Tiff file, calibrated, appropriately scaled, and then cropped into a 768 x 768 pixel
676 square.

677 Each frog was then appropriately scaled and placed randomly onto a leaf litter background. As the
678 number of frogs (n = 360) exceed the number of backgrounds (n = 265), 95 leaf litter images of each
679 distance were randomly selected and rotated by 90˚. The 100 cm images created a Near (N) condition
680 representing close-range viewing conditions, and the 150 cm images generated a Medium (M) viewing
681 condition. To represent even greater viewing distances frogs were randomly reassigned to the 150 cm
682 images and a 16˚ Gaussian filter was applied to remove high spatial frequency information.

683 Eighteen human participants (nine male and nine female, with normal or corrected to normal vision)
684 detected and clicked on frogs on a computer screen (one participant left the study before completing the
685 Far condition). All participants gave their informed consent in line with the Declaration of Helsinki. If a
686 frog could not be detected after 30 s the trial would time out and move to the next image. The speed and
687 accuracy of detection was recorded in *Psychtoolbox* (36) in MATLAB 2015a.

688 Each distance was run as a separate session with participants completing the sessions in a random order
689 separated by a minimum of one hour. Each session contained all 360 stimuli split into 10 blocks of 36
690 images, with participants allowed a short break between each. Stimuli were presented in a separately
691 randomized sequence for each participant.

692 To analyze detection probability data were split into 'correct' and 'incorrect' based on whether the mouse
693 click was within the frog's outline, with a lenience of 10% of the frog's dimensions. Reaction time was
694 log-transformed to normalized distributions. Detection probability was analyzed with a binomial

695 generalized linear mixed effects model and reaction time was analyzed with a general linear mixed effects
696 model (R package *lme4* (37)). Both models included treatment and distance as fixed effects, and
697 participant number as a random factor. Pairwise comparisons of *a priori* interest were calculated in
698 package *multcomp* (38), in R 3.1.3.

699 Pairwise tests were performed to investigate particular hypotheses: i) how the ratio and distribution of
700 color components affects detectability, ii) whether the pattern acts as disruptive camouflage, and iii)
701 whether the natural pattern may act as distance-dependent pattern blending. As the number of pairwise
702 comparisons (11) was equal to the number of degrees of freedom (11), p values did not need to be
703 adjusted.

704 As all manipulated color patterns were generated from standardized colors and effectively posterized, all
705 pairwise comparisons were made to treatment A. To control for the posterization of the pattern during
706 color manipulation treatments A and L were compared.

707 Treatment A was compared to treatments B, C, and D to investigate the role of the ratio of yellow to
708 black. These comparisons investigate how increasing or decreasing the amount of salient yellow pigment
709 could affect the detectability of the frog, i.e. would the frog be able to increase or decrease its
710 detectability by changing the ratio of these two pattern components.

711 As there may be metabolic costs or constraints associated with changing the ratio of pattern components,
712 i.e. the availability of the carotenoid pigments. Treatments E and F represent hypothetical high
713 conspicuous pattern arrangements which maintain the ratio of color components. Treatment E is the
714 largest patch of conspicuous yellow, and F uses the yellow to highlight the edge, and therefore extenuate
715 the recognizable outline of the frog. By comparing A to E and F we investigate whether the natural
716 arrangement of the pattern is optimized for high detectability.

717 High contrast patterning has been linked to breaking up the outline of a target: disruptive camouflage. We
718 tested potential disruptive camouflage effects by comparing treatment G to B (the effect of adding brown

patterning to the plain blue-black), and treatment H to J (the effect of adding blue-black patterning to the plain brown). Disruption would suggest that the contrasting patterns (G and H) should be harder to detect than plain patterns (B and J).

To investigate distance-dependent pattern blending, we tested whether the frog's average color (I) was camouflaged. Firstly, we compared treatments A and I, to see whether the detectability of the frog converged with its mean color as distance increased. We also compared treatment I to the mean color of the background (J) and to background matching camouflage (K). If the frog's average color provides effective camouflage we would expect there to be little difference in reaction time between I, J, and K. Although homogenous colors have been repeatedly demonstrated to provide poor camouflage at close range when compared to textured patterns like K, the mean color of the frog only needs to be effective at greater distances.

731 **References**

732 74 Grimaldi M, Riéra B (2001) Geography and Climate. *Nouragues: Dynamics and Plant-Animal*
733 *Interactions in a Neotropical Rainforest*, eds Bongers F, Charles-Dominique P, Forget P-M, Théry M
734 (Springer Netherlands, Dordrecht), pp 9-18.

735 75 Hurvich LM, Jameson D (1957) An opponent-process theory of colour vision. *Psychol. Rev*. 64:384-
736 404.

737 76 Kelber A (2016) Colour in the eye of the beholder: receptor sensitivities and neural circuits
738 underlying colour opponency and colour perception. *Curr. Opin. Neurobiol*. 41:106-112.

739 77 Vorobyev M, Osorio D (1998) Receptor noise as a determinant of colour thresholds. *Proc. R. Soc. B.*
740 265:351-358.

741 78 Goldsmith TH, Butler BK (2005) Color vision of the budgerigar (*Melopsittacus undulatus*): hue
742 matches, tetrachromacy, and intensity discrimination. *J. Comp. Physiol. A* 191:933-951.

743 79 Barnett JB, Cuthill IC (2014) Distance-dependent defensive coloration. *Curr. Biol.* 24:R1157-R1158.

744 80 Barnett JB, Scott-Samuel NE, Cuthill IC (2016) Aposematism: balancing salience and camouflage.
745 *Biol. Lett.* 12:20160335.

746 81 Xiao F, Cuthill IC (2016) Background complexity and the detectability of camouflaged targets by
747 birds and humans. *Proc. R. Soc. B.* 283:20161527.

748 82 Smith VC, Pokorny J (1975) Spectral sensitivity of the foveal cone photopigments between 400 and
749 500 nm. *Vision Res.* 15:161-171.

750 83 Calderone JB, Jacobs GH (2003) Spectral properties and retinal distribution of ferret cones. *Vis.*
751 *Neurosci*. 20:11-17.

752 84 Macedonia JM, et al. (2009) Conspicuousness of Dickerson's collared lizard (*Crotaphytus*
753 *dickersonae*) through the eyes of conspecifics and predators. *Biol. J. Linn. Soc*. 97:749-765.

754 85 Hart NS (2002) Vision in the peafowl (Aves: *Pavo cristatus*). *J. Exp. Biol.* 205:3925-3935.

755 86 Hart NS, Partridge JC, Cuthill IC (1998) Visual pigments, oil droplets and cone photoreceptor
756 distribution in the European starling (*Sturnus vulgaris*). *J. Exp. Biol.* 201:1433-1446.

757 87 Master TL (1999) Predation by rufous motmot on black and green poison frog. *Wilson Bull.* 111:439-
758 440.

759 88 Alvarado JB, Alvarez A, Saporito RA (2013) *Oophaga pumilio* (strawberry poison frog): predation.
760 *Herpetol. Rev.* 44:298.

761 89 Willink B, García-Rodríguez A, Bolaños F, Pröhl H (2014) The interplay between multiple predators
762 and prey colour divergence. *Biol. J. Linn. Soc.* 113:580-589.

763 90 Hart NS, Hunt DM (2007) Avian visual pigments: characteristics, spectral tuning, and evolution. *Am.*
764 *Nat.* 169:S1-S26.

765 91 Ödeen A, Håstad O (2013) The phylogenetic distribution of ultraviolet sensitivity in birds. *BMC Evol.*
766 *Biol*. 13:36.

92 Myers CW, Daly JW, Malkin B (1978) A dangerously toxic new frog (*Phyllobates*) used by Emberá Indians of Western Colombia, with discussion of blowgun fabrication and dart poisoning. *Bull. Am. Mus. Nat. His.* 161:311-365.

93 Jacobs GH (2009) Evolution of colour vision in mammals. *Philos. Trans. R. Soc. B.* 364:2957-2967.

94 Simões BF, et al. (2016) Multiple rod–cone and cone–rod photoreceptor transmutations in snakes: evidence from visual opsin gene expression. *Proc. R. Soc. B.* 283:20152624.

95 Dreher CE, Cummings ME, Pröhl H (2015) An analysis of predator selection to affect aposematic coloration in a poison frog species. *PLOS ONE* 10:e0130571.

96 Maan ME, Cummings ME (2012) Poison frog colors are honest signals of toxicity, particularly for bird predators. *Am. Nat.* 179:E1-E14.

97 Kelber A, Vorobyev M, Osorio D (2003) Animal colour vision - behavioural tests and physiological concepts. *Biol. Rev.* 78:81-118.

98 Théry M (2001) Forest light and its influence on habitat selection. *Plant Ecol.* 153:251-261.

99 Torgo L (2010) Data mining with R, learning with case studies (Chapman and Hall / CRC, Boca Raton, FL, USA).

100 Field DJ (1987) Relations between the statistics of natural images and the response properties of cortical cells. *J. Opt. Soc. Am. A.* 4:2379-2394.

784 101 Gabor D (1946) Theory of communication. *J. I. Electr. Eng*. 93:429-441.

785 102 Michalis C, Scott-Samuel NE, Gibson DP, Cuthill IC (2017) Optimal background matching
786 camouflage. *Proc. R. Soc. B.* 284:20170709.

787 103 Meyer D, Dimitriadou E, Hornik K, Weingessel A, Leisch F (2017) e1071: Misc Functions of the
788 Department of Statistics, Probability Theory Group (Formerly: E1071), TU Wien. R package version
789 1.6-8. https://cran.r-project.org/package=e1071.

790 104 Lantz B (2013) Machine learning with R (Packt Publishing Ltd., Birmingham, UK).

791 105 Robin X, et al. (2011) pROC: an open-source package for R and S+ to analyze and compare ROC
792 curves. *BMC Bioinformatics* 12:77.

793 106 Merilaita S, Tullberg BS (2005) Constrained camouflage facilitates the evolution of conspicuous
794 warning coloration. *Evolution* 59:38-45.

795 107 Rojas B, Endler JA (2013) Sexual dimorphism and intra-populational colour pattern variation in the
796 aposematic frog *Dendrobates tinctorius*. *Evol. Ecol.* 27:739-753.

797 108 Therneau TM (2015) coxme: mixed effects cox models. R package version 2.2-5. http://cran.r-
798 project.org/package=coxme.

799 109 Brainard DH (1997) The psychophysics toolbox. *Spat. Vis*. 10:433-436.

800 110 Bates D, Maechler M, Bolker B, Walker S (2015) lme4: linear mixed-effects models using Eigen and
801 S4. R package version 1.1-9. http://cran.r-project.org/package=lme4.

802 111 Hothorn T, Bretz F, Westfall P (2008) Simultaneous inference in general parametric models. *Biom. J.*
803 50:346-363.

804

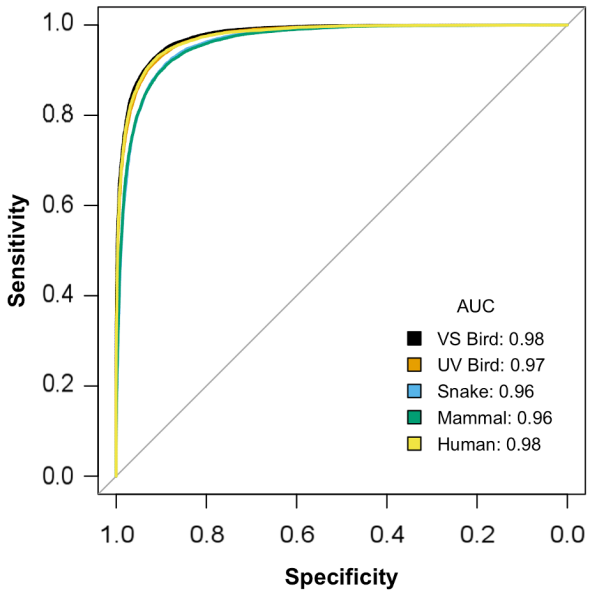

112

113 **Fig. S1.** Discrimination (frog vs background: n = 84) accuracy (Area Under the Curve (AUC) of Receiver Operated Characteristic (ROC) curves from Support Vector Machine (SVM) classification) using all spatiochromatic information (equivalent of close range viewing). All visual systems (VS bird – *Pavo cristatus*, UV bird - *Sturnus vulgaris*, snake - *Masticophis flagellum*, mammal - *Mustela putorius*, and human) were *excellent* at discriminating frogs from backgrounds with near perfect classification. At close range, therefore, the frogs' color and patterning are highly salient and easily

distinguished from the background. AUC of 1.0 equals perfect classification and 0.5 indicates random chance: 1.0-0.9 = excellent, 0.9-0.8 = good, 0.8-0.7 = fair, 0.7-0.6 = poor, 0.6-0.5 = fail (see Table 1).

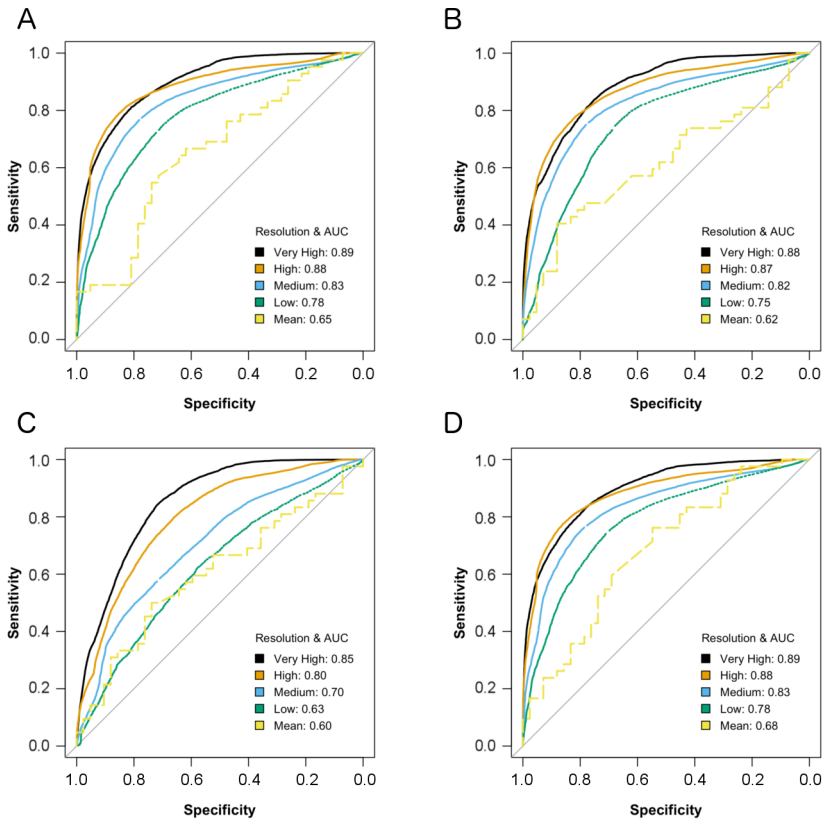

114

115 **Fig. S2.** Color discrimination (frog vs background: n = 84) accuracy (Area Under the Curve (AUC) of Receiver Operated Characteristic (ROC) curves from Support Vector Machine (SVM) classification) at four different spatial resolutions (Very High = close range, Low = long distance) and for the mean color (long distance). Each visual model (A = UV bird: *Sturnus vulgaris*, B = snake: *Masticophis flagellum*, C = mammal: *Mustela putorius*, and D = human) is *good* at discriminating frogs from their backgrounds at close range (Very High), but accuracy declines to *poor* at the furthest distance (Mean). At close range the frog is easily detected, but as distance increases the frogs' colors blend together to more closely match the background and it is harder to distinguish the frog from the

823 background. AUC of 1.0 equals perfect classification and 0.5 indicates random chance: 1.0-0.9 =

824 excellent, 0.9-0.8 = good, 0.8-0.7 = fair, 0.7-0.6 = poor, 0.6-0.5 = fail (Table 1).

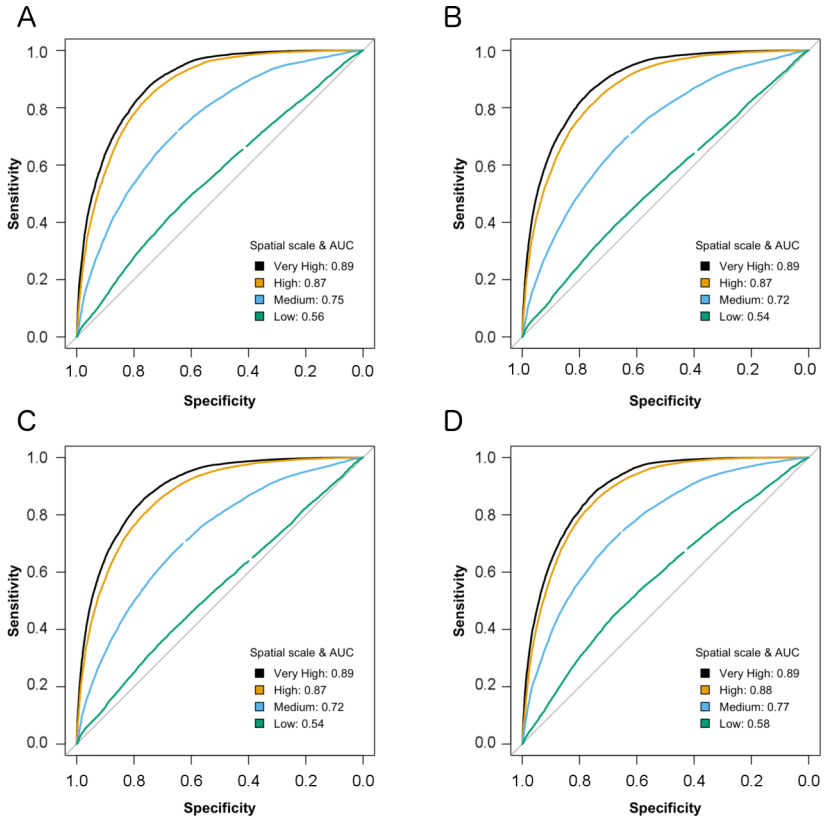

825 116

826 117 **Fig. S3.** Visual texture discrimination (frog vs background: n = 84) accuracy (Area Under the Curve
827 (AUC) of Receiver Operated Characteristic (ROC) curves from Support Vector Machine (SVM)
828 classification) at four different spatial resolutions (Very High = close range, Low = long distance).
829 For each visual model (A = UV bird: *Sturnus vulgaris*, B = snake: *Masticophis flagellum*, C =
830 mammal: *Mustela putorius*, and D = human), discrimination accuracy declines from *good* at close
831 range (Very High) to *fail* at the furthest distance (Low). At close range the patterning of the frog,
832 independent of coloring, is easily distinguished from the visual texture distribution of the background,
833 but as distance increases the frog becomes harder to classify. AUC of 1.0 equals perfect classification
834 and 0.5 indicates random chance: 1.0-0.9 = excellent, 0.9-0.8 = good, 0.8-0.7 = fair, 0.7-0.6 = poor,
835 0.6-0.5 = fail (Table 1).

836 118

Fig. S4. Examples of the stimuli used in the survival experiment. Three different frog colors were presented to four different backgrounds. Frogs colors: C: brown-and-black (camouflage), Y: plain yellow (aposematism), and N: the natural yellow-and-black pattern. Backgrounds: NL: natural leaf litter, NS: natural soil (leaf litter removed), PL: paper printed with photograph of leaf litter, and PA: paper printed with homogeneous color (mean of PL).

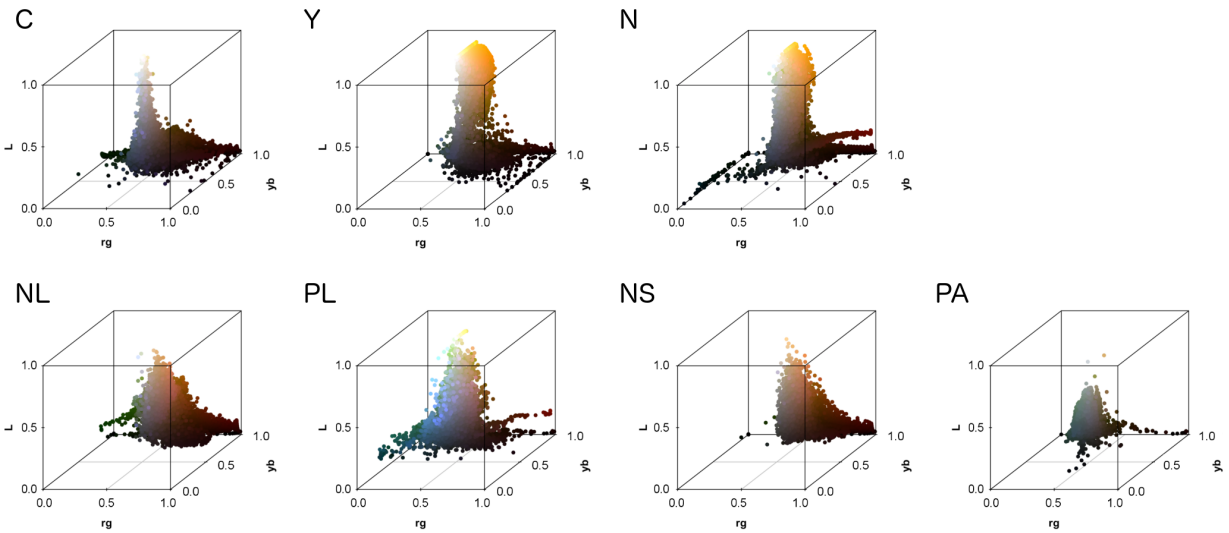

121

122 **Fig. S5.** Avian (VS - *Pavo cristatus*) visual modeling of each plasticine frog (top) and each background (bottom) used in the survival experiment (see Fig. S4 for photographs). C – brown and black frog (camouflage: n = 14), Y – yellow frog (aposematism: n = 15), N – yellow and black frog (natural pattern: n = 14), NL - natural leaf litter background (n = 19), PL – printed leaf litter background (n = 19), NS - natural soil background (n = 20), and PA – printed average background (n = 20). The yellow component of the plain yellow (Y) and natural patterned (N) frogs is an obvious outlier from all backgrounds (NL, PL, NS, and PA), whereas the brown-and-black frog (C) is a closer match to the natural background (NL) than to the modified background (PA).

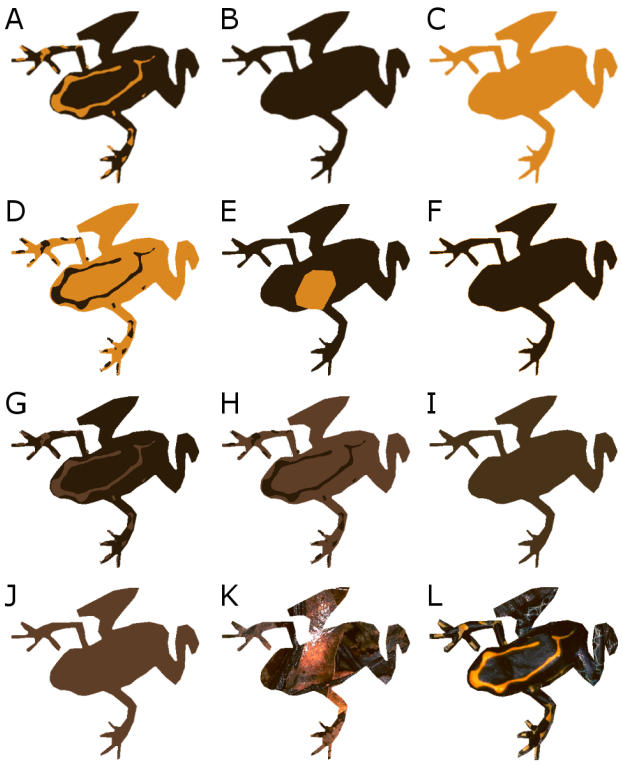

Fig. S6. Examples of the stimuli used in the detection experiment. Each set of 12 treatments was based on a different frog (n = 30). Standardized frog colors (A, B, C, D, E, F, G, H, & I) were created using *k*-means clustering the RGB color space into four clusters (yellow = centroid with the highest ratio of R+G to B; blue-black = centroid with lowest luminance). A: posterized natural pattern using standardized colors, B: plain blue-black, C: plain yellow, D: reversed color natural pattern, E: all yellow pixels of A grouped into one approximately circular patch, F: all yellow pixels from A moved to the frog's edge, G: natural pattern with yellow replaced with the mean color of the background, H: inverse of pattern G, I: mean color of the frog, J: mean color of the background, K: background matching camouflage (random sample of leaf litter background), and L: unmanipulated natural frog pattern.